Origin of Rotation and Inversion Barriers

R. F. W. Bader,*,† J. R. Cheeseman,† K. E. Laidig,† K. B. Wiberg,‡ and C. Breneman‡

Contribution from the Department of Chemistry, McMaster University, Hamilton, Ontario, L8S 4M1 Canada, and Department of Chemistry, Yale University, New Haven, Connecticut 06511. *Received November 1, 1989*

Abstract: This paper discusses the origin of barriers to rotation and inversion at the SCF and CI levels by use of the theory of atoms in molecules. The barriers are related to the changes in the attractive and repulsive potential energies through the use of the virial theorem. Rotation barriers in C_2H_6, CH_3OH, and CH_3NH_2 are shown to result from an increase in the attractive potential energy and in spite of a decrease in the repulsive energy. Just the opposite behavior is found for the inversion barriers in NH_3, PH_3, and H_3O^+ and for the barrier to bending in H_2O. The relative changes in energy found for the rotation barriers are anticipated for conformational changes dominated by an increase in internuclear separations, while those for the inversion barriers are typical of changes accompanied by decreases in these separations. The origins of the barriers are given in terms of the mechanical properties of the atoms. In ethane, the transformation of a S_3 to a C_3 symmetry axis in attaining the eclipsed geometry induces a quadrupole polarization of the density in the C–C bond, causing it to lengthen. This lengthening leads to a decrease in the magnitude of the attractive interaction of each carbon nucleus for the electronic charge in the basin of the other carbon atom, and this is the origin of the barrier. The changes in the charge distribution that determine these changes in atomic properties are not consistent with a model that relates the barrier in this molecule to Pauli-like exchange repulsions between localized C–H bond orbitals.

Introduction

The prediction and understanding of changes in energy are among the most important challenges in chemistry. Quantum mechanics predicts the change in energy accompanying a change in state for the total system and for every atom in the system.[1,2] The atomic view of a system's properties increases our understanding of the mechanics of a process and aids in our attempts to construct predictive models. In addition to predicting the total energy, quantum mechanics enables one to calculate the average values of the kinetic and potential energy contributions, the latter consisting of the nuclear–electron attractive potential energy (V_{ne}) and the electron–electron and the nuclear–nuclear repulsive energies (V_{ee} and V_{nn}, respectively). These energies, along with the contribution to the potential energy of the electrons arising from the virials of the external forces exerted on the nuclei,[1] are the only energy quantities defined in terms of the usual fixed-nucleus Hamiltonian in the absence of external fields. Model-independent predictions and interpretations of energy changes are, therefore, restricted to these quantities and the atomic contributions to these quantities. The theory of atoms in molecules, since it enables one to calculate all well-defined mechnical properties at the atomic level, places new emphasis on the study of these energies.

The electron–nuclear interaction energy is the only attractive interaction in a molecular system, and it is the decrease in the potential energy resulting from this interaction that is responsible for the formation of a bound molecular state from the separated atoms. In the absence of external forces acting on the nuclei, the virial theorem states that the total energy E equals $(1/2)V$, where $V = V_{ne} + V_{ee} + V_{nn}$ is the total potential energy. Similarly, the change in energy ΔE between two states free of external forces equals $(1/2)\Delta V$. Energy changes associated with relatively large reductions in internuclear separations, such as those enountered in the formation of molecules from atoms, lead to a decrease in the attractive potential energy and to increases in the electron–electron and nuclear–nuclear energies of repulsion. The attractive potential energy, however, does not necessarily decrease when the total energy decreases. Thus, it is possible for the total energy to decrease and for a system to become more stable in spite of an increase in attractive potential energy because of an even larger reduction in the energies of repulsion. Correspondingly, it is possible for the energy to increase and for a system to become less stable in spite of a decrease in the attractive energy.

One anticipates that the changes in the electron–electron and nuclear–nuclear repulsions will, in general, parallel one another. It is frequently found, as anticipated on simple grounds, that the changes in the repulsive energies V_{ee} and V_{nn} are nearly equal and that each is approximately half the magnitude of the change in the attractive potential energy. Consider the formation of AB from neutral atoms A and B. The new interactions, without charge transfer, are as follows: nuclear repulsion, Z_aZ_b/R; electron repulsion, $\approx N_aN_b/R$ $(=Z_aZ_b/R)$; electron–nuclear attractive energy, which is approximately equal to the negative sum of the two interactions, $\approx -(Z_aN_b/R + Z_bN_a/R)$. The same near-cancellation occurs when there is a transfer of charge A → B, but to the same order of approximation, one must include the change in the internal energies, a change that is approximated by $-I_a + A_b$ where I is an ionization potential and A an electron affinity. Thus, whether a nuclear displacement results in an increase or a decrease in the total energy is determinated by the difference in larger competing changes in the attractive and repulsive potential energies, changes that are approximately equal in magnitude.

Other decompositions of the total energy have been suggested. Allen[3a] introduced the terms attractive and repulsive dominant in the classification of barriers, with the attractive and repulsive contributions defined, respectively, as V_{ne} and $(T + V_{ee} + V_{nn})$. Payne and Allen[3b] discuss this and other partitionings of the energy in a review of barrier calculations done in the seventies. Csizmadia[4] has discussed the separate contributions of V_{nn} and the remaining energy terms $(T + V_{ne} + V_{ee})$, which he calls the electronic contribution, to energy barriers. These early results were criticized[3b,5] because of an apparent dependence of the resulting interpretation on the basis set. These sets were small, and difficulties in interpreting these early studies were further compounded by the use of unoptimized geometries. As is demonstrated here, these criticisms do not apply when one uses basis sets of a size sufficient to describe the accompanying relaxations in the charge density and optimized geometries are employed for the energy maxima and minima. In addition, the use of the virial theorem for the basis of the partitioning, as is done in the present study, enables one to isolate and include the contribution to the virial arising from the forces exerted on the nuclei for other

† McMaster University.
‡ Yale University.

(1) Bader, R. F. W.; Nguyen-Dang, T. T. *Adv. Quantum Chem.* **1981**, *14*, 63.
(2) Bader, R. F. W. *Pure Appl. Chem.* **1988**, *60*, 145.
(3) (a) Allen, L. C. *Chem. Phys. Lett.* **1968**, *2*, 597. (b) Payne, P. W.; Allen, L. C. *Applications of Electronic Structure Theory*; Schaefer, H. F., Ed.; Plenum: New York, 1977; pp 29–108.
(4) Csizmadia, I. G. *Theory and Practice of MO Calculations on Organic Molecules*; Elsevier: New York, 1976.
(5) Veillard, A. *Internal Rotation in Molecules*; Orville-Thomas, W. J., Ed.; Wiley: New York, 1974; pp 385–424.

0002-7863/90/1512-6530$02.50/0

Table I. Dissociation, Rotation, and Inversion Barriers[a]

molecule	E, au	$\gamma = -V/T$	ΔE	ΔV_a, au	ΔV_r, au	ΔV_{nn}, au	ΔV_{ee}, au	ΔE(exptl)
				Dissociation[b]				
N_2	−109.298 81	1.998 74	8.0	48.1548	−47.5673	−24.2972	−23.2701	9.91[d]
BF	−124.438 59	2.000 73	6.9	38.0201	−37.5096	−19.1076	−18.4019	7.90[d]
LiF	−107.222 69	2.000 88	5.5	20.6530	−20.2499	−9.1466	−11.1032	5.97[d]
				Internal Rotation[c]				
C_2H_6	−79.257 33	2.000 26	3.0	0.3321	−0.3223	−0.1687	−0.1537	2.93[e]
CH_3NH_2	−95.251 67	2.000 34	2.0	0.1627	−0.1562	−0.0840	−0.0722	1.98[f]
CH_3OH	−115.086 44	2.000 54	1.0	0.0938	−0.0906	−0.0492	−0.0414	1.07[g]
				Inversion[j]				
NH_3	−56.436 95	1.999 50	5.4	−0.2058	0.2232	0.1043	0.1189	5.8[h]
PH_3	−342.649 92	1.999 97	34.2	−0.4875	0.5965	0.3429	0.2536	31.5[i]
H_3O^+	−76.569 23	1.999 89	2.1	−0.1028	0.1094	0.0335	0.0759	
H_2O	−76.293 26	2.000 08	33.0	−0.2345	0.3399	0.1237	0.2162	

[a] The potential energies have been scaled by a factor close to unity to satisfy the virial theorem. [b] 6-311++G(2d,2p)/6-311++G(2d,2p) CI singles and doubles. ΔE values in electronvolts. [c] 6-311++G(2d,2p)/6-311++G(2d,2p). ΔE values in kilocalories per mole. [d] Huber, K. P.; Herzberg, G. *Molecular Spectra and Molecular Structure*; Van Nostrand: New York, 1979. [e] Weiss, S.; Leroi, G. *J. Chem. Phys.* **1968**, *48*, 962. [f] Lide, D. R., Jr. *J. Chem. Phys.* **1941**, *27*, 343. [g] Ivash, E. V.; Dennison, D. M. *J. Chem. Phys.* **1953**, *21*, 1804. [h] Dumbacker, B. *Theor. Chim. Acta* **1972**, *23*, 346. [i] Weston, R. E. *J. Am. Chem. Soc.* **1954**, *76*, 2645. [j] 6-311++G(2d,2p)/6-311++G(2d,2p) CI singles and doubles. ΔE values in kilocalories per mole.

geometries. The interpretations so obtained are stable to changes in the basis set and to the addition of correlation, and no contributions to the electronic potential energy are ignored.

We denote the electron–nuclear attractive potential energy as V_a and the sum of the electron–electron and nuclear–nuclear repulsive energies as V_r. The two possible origins of a barrier as determined by their relative changes are summarized in Figure 1. In case I, there is an increase in total energy E as a result of an increase in V_a and a smaller decrease in V_r, while in case II the increase in E is a result of a decrease in V_a accompanied by an even larger increase in V_r. Also indicated in the figure is the reverse of each process. The reverse of case I, as noted above, is generally associated with significant decreases in internuclear separations, such as the formation of a molecule from separated atoms. Thus, one anticipates that a case I barrier will result from an increase in internuclear separations. Table I lists values of ΔV_a and ΔV_r for the barrier to dissociation of N_2, BF, and LiF obtained from CI calculations that give dissociation energies close to the observed values. The magnitudes of ΔV_{nn} and ΔV_{ee} are nearly equal and each is approximately half of ΔV_{ne}, but overall the increase in V_a exceeds the decrease in V_r and $\Delta E > 0$. The value of V_{nn} is larger for N_2 than for isoelectronic BF, since Z_aZ_b is a maximum when $Z_a = Z_b$. Following similar arguments, one would expect a case II barrier to result from an overall decrease in internuclear separations, leading to the dominance of the repulsive energy increase in such instances.

Considered from the point of view of $\Delta E > 0$, case I is exemplified by barriers to internal rotation and case II by barriers to inversion. We shall discuss the barriers to internal rotation in ethane, methylamine, and methanol as examples of case I and the inversion or bending barriers in NH_3, PH_3, H_3O^+, and H_2O as examples of case II.

Theoretical Calculations

Calculations at the single-determinant level with use of the 6-311++G(2d,2p) basis set[6a] for both geometry optimization and energy determination were performed for all of the molecules. The above basis is the 6-311G** basis[6b] with an extra diffuse s and p set on the heavy atoms and an extra diffuse s function on H, together with a second set of polarizing functions on all atoms. The total energies obtained by Cade and Wahl[7a] for N_2 and by Cade and Huo[7b] for BF and LiF using a very extended set of STO's in calculations that are close to the Hartree–Fock limit are more negative than the SCF energies obtained here by 0.0116 au for N_2, 0.0164 au for BF, and 0.0115 au for LiF. The results reported here for NH_3, PH_3, H_2O, H_3O^+, N_2, BF, and LiF are obtained from configuration interaction calculations, with all single and double configurations generated from the large set of basis functions. In addition, MP2 calculations with the 6-31G** basis were performed for ethane, methylamine, and methanol to ensure that the results obtained for these molecules are also stable to the addition of electron correlation.

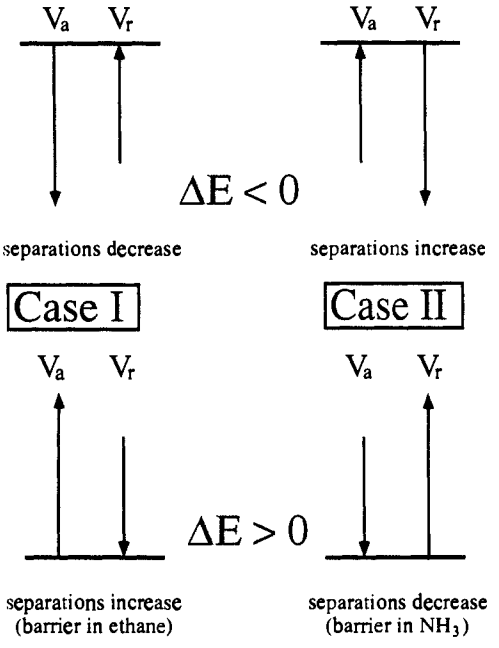

Figure 1. Diagramatic representation of the relative contributions of the changes in the attractive (V_a) and repulsive (V_r) energies to barriers characterized by an increase or decrease in internuclear separations.

The calculated total energies are reported in Table I. Good agreement of the values for rotation and inversion barriers obtained at the SCF level with the experimental values is anticipated on the basis of previous results.[3b] The SCF and correlated energy hypersurfaces for closed-shell systems parallel one another for nuclear motions such as inversions and rotations that do not involve large bond extentions,[8] implying that the correlation energy stays relatively constant for such motions. It is necessary to include polarizing functions in the calculation of inversion barriers because of the significant changes in hybridization that accompany such nuclear motions.[3b,9] The relative values of the contributions to ΔE reported in Table I, as well as the values of ΔE themselves, are stable to changes in basis set or level of calculation. The use of the 6-31G** basis with optimized geometries already recovers all of the results and conclusions reported here; results that are obtained with a much larger basis set and that include electron correlation.

(6) (a) Frisch, M. J.; Pople, J. A.; Binkley, J. S. *J. Chem. Phys.* **1984**, *80*), 3265. Clark, T.; Chandrasekhar, J.; Spitznagel, G. W.; Schleyer, P. v. R. *J. Comput. Chem.* **1983**, *4*, 294. (b) Krishnan, R.; Binkley, J. S.; Seeger, R.; Pople, J. A. *J. Chem. Phys.* **1980**, *72*, 650. McLean, A. D.; Chandler, G. S. *J. Chem. Phys.* **1980**, *72*, 5639.

(7) (a) Cade, P. E.; Wahl, A. C. *At. Data Nucl. Data Tables* **1974**, *13*, 339. (b) Cade, P. E.; Huo, W. M. *At. Data Nucl. Data Tables* **1973**, *12*, 415.

(8) Stanton, R. E. *J. Chem. Phys.* **1962**, *36*, 1298.

(9) Rauk, A.; Allen, L. C.; Clementi, E. *J. Chem. Phys.* **1970**, *52*, 4133.

Table II. Changes in Bond Lengths (Å) and Bond Angles (deg) upon Rotation or Inversion

molecule		bond length or bond angle	Δ^b
C_2H_6	C–C	1.5247	0.0140
	C–Hϵ	1.0835	–0.0010
	∠HϵCC	111.19	0.42
CH_3NH_2[a]	C–N	1.4531	0.0064
	C–H	1.0877	–0.0049
	C–Hϵ	1.0820	0.0012
	N–H	0.9974	–0.0025
	∠HCN	114.36	–3.72
	∠HϵCN	109.36	2.28
	∠CNH	111.07	0.83
CH_3OH[a]	C–O	1.3999	0.0035
	C–Hϵ	1.0791	0.0039
	C–H	1.0850	–0.0030
	O–H	0.9383	–0.0018
	∠HϵCO	107.31	4.63
	∠HCO	111.79	–2.12
	∠COH	110.03	0.60
NH_3	N–H	0.9984	–0.0130
	∠HNH	107.98	12.02
PH_3	P–H	1.4042	–0.3500
	∠HPH	95.47	24.53
H_3O^+	O–H	0.9593	–0.0040
	∠HOH	113.30	6.7
H_2O	O–H	0.9410	–0.0180
	∠HOH	106.31	73.69

[a] Methyl hydrogens that become eclipsed in the rotated conformer are denoted by Hϵ. [b] A positive value denotes an increase in length or angle in attaining the transition-state geometry.

Discussion

Rotational Barriers. The dominant geometry change encountered in the formation of a rotationally eclipsed conformer from a staggered one is an increase in the length of the bond about which rotation occurs. In ethane, the C–C separation increases in forming the eclipsed conformer, and this increase is more than 10 times larger than the accompanying decreases in the C–H separations. The CCH bond angles open by 0.4°, and there is an overall decrease of 0.0069 Å in the separations of the hydrogens on a given carbon. In methylamine and methanol, the C–N and C–O separations also increase upon rotation to the eclipsed conformation, although by smaller amounts than the C–C bond in ethane. The bond lengths of the methyl hydrogens that become eclipsed (labeled as Hϵ in Table II) increase in both molecules, as do the angles they make with the C–N or C–O axis, while the bonds and corresponding angles to the noneclipsed hydrogens undergo a decrease upon rotation. The N–H and O–H bond lengths also undergo a decrease. Unlike ethane, all of the changes in bond lengths are of roughly the same magnitude in methylamine and methanol. Both the predicted pattern of geometrical changes and their magnitudes are maintained at the MP2/6-31G** level of calculation. The MP2 calculations predict increases in the C–C, C–N, and C–O bond lengths upon rotation of 0.0134, 0.0068, and 0.0048 Å, respectively (compare Table II). Reference to Table I shows that these rotational barriers result from an increase in the attractive potential energy and a decrease in the repulsive potential energy, in agreement with the general arguments given above. The atomic origin of the barrier in ethane is presented next.

Rotational Barrier in Ethane. The increase in the C–C separation dominates the changes in V_{nn} and V_{ee} in ethane, as both these quantities undergo decreases of similar magnitude when the staggered (S) is rotated into the eclipsed (E) conformer. The same geometrical increase results in a lessening of the attractive interactions within the molecule, with the increase in V_a exceeding the decrease in the repulsive interactions. Thus, the barrier to internal rotation in ethane results from a reduction in the attractive interactions between the nuclei and the electrons and in spite of an accompanying reduction in the electron–electron and nuclear–nuclear repulsions. The energy changes that give rise to the rotation barrier are characteristic of case I and represent a small reversal of the process of C–C bond formation (Figure 2).

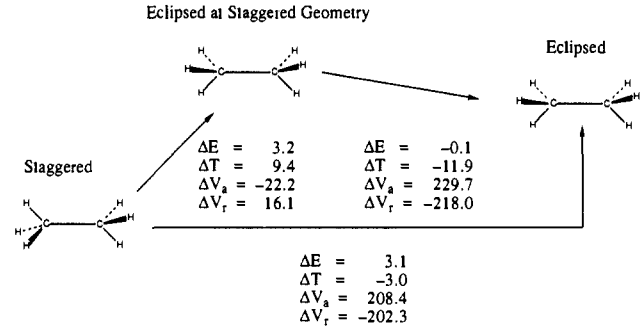

Figure 2. Energy changes for the rotation of the staggered conformer (S) into the eclipsed conformer (E) and into the frozen eclipsed conformer (FE).

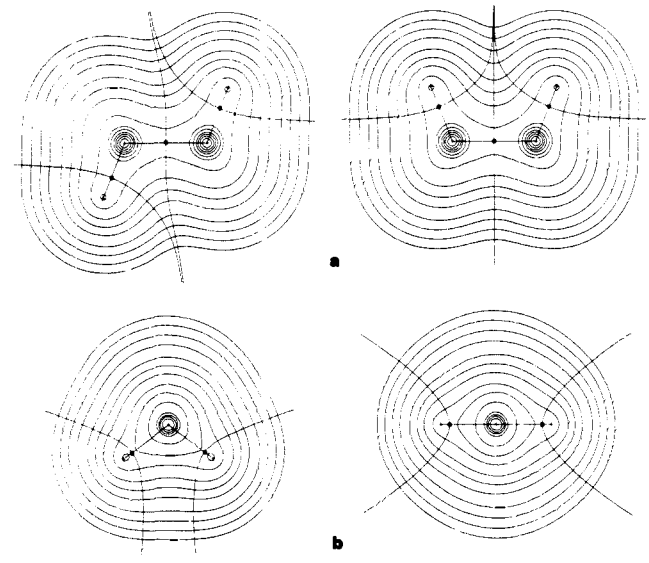

Figure 3. Contour maps of the electronic charge density for the staggered and eclipsed conformers of ethane and for the bent and linear conformers of water. The outermost contour has the value 0.001 au. The remaining contours increase in value in the order 2×10^n, 4×10^n, and 8×10^n beginning with $n = -3$ and increasing in steps of unity to give a maximum contour of 20 au. The bond paths, the interatomic surfaces, and the bond critical points are also indicated.

The changes in the charge distribution of ethane caused by the internal rotation are relatively small (Figure 3). The principal change is the replacement of the slightly curved C–C interatomic surface in the S conformer with the planar one of the E conformer, a consequence of the replacement of a threefold alternating axis of symmetry with a simple threefold axis. With reference to Figure 3, one sees that the upper arm of the atomic surface of an eclipsed hydrogen atom is moved inward relative to its form in the S conformer and the volume of a hydrogen atom that equals 38.44 au in the S geometry is slightly decreased, by 0.24 au. The remainder of the basin of a hydrogen atom is nearly unperturbed by the rotation. The changes in ρ at the bond critical points[10] are small, being largest for the C–C bond for which the value of ρ_b decreases by 0.0071 au from a value of 0.2495 au in the S conformer. Its value for the C–H bond increases by 0.0008 au from its value of 0.2908 au. The C–H bond critical point shifts by 0.0017 au toward the proton in the eclipsed geometry, a harbinger of the small transfer of charge from H to C that accompanies the rotation. The C–H bonds in ethane exhibit a small ellipticity[10] with major axes directed so as to be tangent to the cone obtained by rotation of the C–H bonds of a methyl group about the C–C axis. This ellipticity approximately doubles in value to 0.014 when the group is rotated into the eclipsed geometry.

(10) Bader, R. F. W.; Slee, T.; Cremer, D.; Kraka, E. *J. Am. Chem. Soc.* **1983**, *105*, 5061.

Table III. Atomic Contributions to Barriers[a]

molecule	Ω	$E(\Omega)$	$q(\Omega)$	$\Delta E(\Omega)$	$\Delta N(\Omega)$	$\Delta V_a(\Omega)$	$\Delta V_r(\Omega)$	$\Delta V_a°(\Omega)$	r_H[b]	Δr_H
N_2	N	−54.649 40	0.000	92.2	0.000	24.0774	−23.7836	1.4239		
	$\sum_\Omega \Delta E(\Omega)$			184.4						
BF	B	−24.212 99	0.902	−239.3	0.902	10.8928	−11.6554	−2.2924		
	F	−100.225 59	−0.902	399.4	−0.902	27.1239	−25.8508	5.7786		
	$\sum_\Omega \Delta E(\Omega)$			160.1						
LiF	Li	−7.362 70	0.932	−43.5	0.932	5.4975	−5.6362	−0.7821		
	F	−99.859 95	−0.932	170.0	−0.932	15.1559	−14.6141	5.1026		
	$\sum_\Omega \Delta E(\Omega)$			126.5						
C_2H_6	C	−37.672 15	0.184	2.6	0.010	0.0878	−0.0802	−0.0135		
	H	−0.652 24	−0.0612	−0.3	−0.003	0.0261	−0.0270	0.0012	0.7766	−0.0017
	$\sum_\Omega \Delta E(\Omega)$			3.4						
NH_3	N	−54.917 46	−1.005	−36.5	0.145	−0.8874	0.7711	−0.5634		
	H	−0.506 49	0.335	14.0	−0.048	0.2274	−0.1829	0.0468	0.5112	−0.0226
	$\sum_\Omega \Delta E(\Omega)$			5.5						
PH_3	P	−340.271 67	1.546	3.2	0.131	−0.9957	1.0060	−0.4207		
	H	−0.792 91	−0.515	10.3	−0.044	0.1696	−0.1367	0.0426	1.2958	−0.0422
	$\sum_\Omega \Delta E(\Omega)$			34.1						
H_3O^+	O	−75.765 05	−1.222	−18.9	0.047	−0.3720	0.3117	−0.2668		
	H	−0.268 05	0.741	7.0	−0.016	−0.0898	−0.0675	0.0220	0.2959	−0.0071
	$\sum_\Omega \Delta E(\Omega)$			2.1						
H_2O	O	−75.539 33	−1.172	−101.1	0.310	−1.8776	1.5552	−1.3985		
	H	−0.376 97	0.586	67.1	−0.155	0.8223	−0.6085	0.2066	0.3447	−0.0604
	$\sum_\Omega \Delta E(\Omega)$			33.1						

[a] All results in atomic units except for ΔE values which are in kilocalories per mole. [b] r_H is the bonded radius of hydrogen.

Thus, the extent to which electronic charge is accumulated in the tangent plane containing the C–H bond as opposed to the one perpendicular to it, while small, is increased when the molecule attains the staggered geometry.

The atomic contributions to the energy changes are given in Table III. The changes in the energies of the individual atoms are small, a reflection of the small perturbations of the atomic charge distributions that accompany the internal rotation. The net charge on a H atom in the staggered form is $q(H) = -0.061e$. On changing to the eclipsed geometry, there is a transfer of 0.003e from each hydrogen to the carbons. Each H atom is stabilized by a small amount in the eclipsed geometry in spite of the small decrease in its population. Each carbon atom is destabilized by an amount nine times the magnitude of the stabilization of the hydrogens bonded to it, and this is the source of the barrier at the atomic level. The transfer of charge to C leads to a decrease in $V_a°(C)$, the potential energy of interaction of the C nucleus with its own charge distribution, with $\Delta V_a°(C) = -8.5$ kcal/mol. The energy change for C, however, is dominated by the increase in the C–C separation. This increase, while leading to a reduction in the repulsive interactions between the two C atoms, gives rise to an even greater reduction in the attractive interaction of each C nucleus with the charge density on the other C atom. ($\Delta V_a(C)$ consists of $\Delta V_a°(C)$, which is less than zero, and the interaction of each of the other nuclei with the charge density of the carbon atom in question. Since the C–H bond lengths have decreased in the eclipsed geometry and only the C–C length has increased, the increase in $V_a(C)$ is the result of the latter effect.) Thus, the carbon atoms are destabilized in the eclipsed geometry as a result of a decrease in the attractive interactions of each carbon nucleus with the charge density of the other. These energy changes of the carbon atom dominate the change in energy for the total system, and hence the barrier in ethane is an example of case I.

Orbital arguments concerning the origin of the barrier to rotation in ethane have been reviewed and discussed by Pitzer.[11] The explanation favored by him is based on a model in which the molecular orbitals for the staggered geometry are first frozen in form and the nuclear framework of the staggered geometry is rotated without change into the eclipsed geometry. This leads to a small negative barrier, a result that is interpreted to mean that simple electrostatic interactions between the ends of the molecule are not important in the ethane barrier. The freezing of the orbitals destroys their orthogonality, which is required by the Pauli principle, and the change in ρ obtained from their reorthogonalization results in so-called overlap or exchange repulsion contributions to the energy,[12] that is, to so-called "Pauli repulsions" between the C–H bond orbitals. Changes in the nuclear–electron and Coulomb integrals make the largest contributions to the potential energy change, resulting from this change in density.[11] The energy change could, therefore, be the result of an increase in V_a or of a decrease in V_r. Equating a repulsive interaction to the overlap of occupied orbitals and an attractive one to the overlap between filled and vacant orbitals has been used by a number of authors to account for rotational barriers.[13,14] This interpretation has been recently used by Dorigo et al.[15a] and by Carpenter and Weinhold.[15b,c] The two latter papers include extensive discussions of the effects of geometry optimization on rotation barriers.

Imposing orthogonality on some initial set of model orbitals and equating the changes in the model density to the requirements of the Pauli principle have been used previously to define "Pauli repulsions"[16] as found, for example, in the He_2 repulsive interaction or as evisaged in the VSEPR model of molecular geometry.[17] The difficulty with such models is that the answer one obtains is determined by one's choice of the original set of orbitals. This is illustrated by the work of Corcoran and Weinhold,[18] who showed that it is possible to pick a set of C–H bond orbitals almost identical with the set used in the Pauli repulsion model[11,12] in their final orthogonalized form, but predicting an ethane rotation barrier of incorrect sign when used in an antisymmetric wave function assuming a tetrahedral rigid-rotor geometry.

While, as shown in Figure 3, the charge distribution of ethane changes so that the basins of the eclipsed hydrogen atoms do not overlap in forming the E conformer, these changes in ρ do not correspond to a compression of the hydrogen atoms. A pair of eclipsed hydrogens do not share a common interatomic surface, and thus they do not touch as occurs in a closed-shell repulsion.

(11) Pitzer, R. M. *Acc. Chem. Res.* **1983**, *16*, 207.

(12) Sovers, O. J.; Kern, C. W.; Pitzer, R. M.; Karplus, M. *J. Chem. Phys.* **1968**, *49*, 2592.

(13) Gimarc, B. M. *Molecular Structure and Bonding*; Academic: New York, 1979, p 148ff.

(14) Lowe, J. P. *Prog. Phys. Org. Chem.* **1968**, *6*, 1. Lowe, J. P. *Science (Washington, D.C.)* **1973**, *179*, 527. Brunck, T. K.; Weinhold, F. *J. Am. Chem. Soc.* **1979**, *101*, 1700.

(15) (a) Dorigo, A. E.; Pratt, D. W.; Houk, K. N. *J. Am. Chem. Soc.* **1987**, *109*, 6591. (b) Carpenter, J. E.; Weinhold, F. *J. Phys. Chem.* **1988**, *92*, 4306. (c) Carpenter, J. E.; Weinhold, F. *J. Mol. Struct. THEOCHEM* **1988**, *169*, 41.

(16) Bader, R. F. W.; Preston, H. J. T. *Can. J. Chem.* **1966**, *44*, 1131.

(17) Gillespie, R. J. *Molecular Geometry*; Van Nostrand Reinhold: London; 1972.

(18) Corcoran, C. T.; Weinhold, F. *J. Chem. Phys.* **1980**, *72*, 2866.

This is reflected in the decrease in the repulsive contributions to their energy (Table III). Instead, the spatial extent of each hydrogen atom is diminished by a transfer of a small portion of its space and its contained charge to the carbon atoms, each of whose volumes increases by 0.47 au.

To demonstrate that the increased C–C bond length in the E conformer and hence the barrier are not a result of repulsions between eclipsed hydrogens, one can inquire into the origin of the barrier resulting from an internal rotation of the rigid nuclear framework of ethane from its staggered to an eclipsed geometry, and do so without recourse to a model state. Such a configuration of the nuclei, while physically realizable, does not lie on the reaction path, and it possesses an energy slightly in excess of the eclipsed transition-state geometry. Forces act on the nuclei in this constrained geometry such as to move them into the positions they occupy in the eclipsed transition state. Since the major geometrical change between the staggered and eclipsed equilibrium geometries is a lengthening of the C–C bond, one anticipates that the principle forces operative in the frozen eclipsed geometry are forces of repulsion acting on the two carbon nuclei. The changes in the potential and kinetic energies for the nuclear motions staggered to frozen eclipsed, S → FE, frozen eclipsed to eclipsed, FE → E, and S → E are summarized in Figure 2.

Because forces act on the nuclei in the FE conformation, the general statements of the virial theorem, which include the contributions of the virials of the nuclear forces to the total electronic energy, must be used.[19] The contribution of nucleus α to the virial of the forces acting on the electrons is equal to $-\mathbf{X}_\alpha\cdot\mathbf{F}_\alpha$, where $\mathbf{X}_\alpha$ is the position vector of nucleus α and $\mathbf{F}_\alpha = -\nabla_\alpha E$, the net force acting on it. The general statement of the virial theorem is

$$2T = -\Lambda = -V + \sum_\alpha \mathbf{X}_\alpha\cdot\mathbf{F}_\alpha \tag{1}$$

where Λ, the virial of the forces exerted on the electrons, is the potential energy of the electrons. When the forces on the nuclei vanish, $\Lambda = V = V_a + V_r$, and one obtains the corresponding statements of the virial theorem, $T = -E$ and $E = (1/2)V$. The general statement corresponding to $T = -E$ is

$$T = -E + \sum_\alpha \mathbf{X}_\alpha\cdot\mathbf{F}_\alpha \tag{2}$$

When the nuclear virial is positive, T must exceed $|E|$ to balance the contribution to the virial arising from the repulsive forces acting on the nuclei. Since we are taking differences between a state where the forces do not vanish and one where they do, the total nuclear virial for the nonequilibrium state appears in the difference. Thus, for the reaction S → FE, the change in kinetic energy equals minus the change in total energy plus the nuclear virial:

$$\Delta T = -\Delta E + \sum_\alpha \mathbf{X}_\alpha\cdot\mathbf{F}_\alpha \tag{3}$$

Since ΔT is positive for the reaction S → FE (Figure 2) and exceeds the magnitude of ΔE, the nuclear virial is positive, showing that this contribution to the potential energy of the electrons is dominated by repulsive forces acting on the nuclei. The corresponding expression for the change in potential energy is

$$\Delta V = \Delta V_a + \Delta V_r = 2\Delta E - \sum_\alpha \mathbf{X}_\alpha\cdot\mathbf{F}_\alpha \tag{4}$$

In this case, V_a decreases and V_r increases, both quantities changing in the direction opposite to that for the overall reaction S → E, but the increase in repulsive energy arising from the nuclear–nuclear and electron–electron forces is less than the decrease in the attractive potential energy, and overall the change in the potential energy is less than zero; i.e., the attractive contributions dominate. *Thus, the increase in energy encountered in the formation of the frozen eclipsed conformer comes not from an increase in the usual potential energy contributions but from the virials of the repulsive forces acting on the carbon nuclei in the nonequilibrium geometry.* This is also evident in the expression for the total energy change expressed as $\Delta E = \Delta T + \Delta V$. The fact that $\Delta T > \Delta E$ shows that ΔT includes the contribution of a repulsive nuclear virial. The atomic contributions to the change S → FE, like those for S → E, come primarily from the carbon atoms, $\Delta T(C) = 4.0$ kcal/mol and $\Delta V_a(C) = -35.8$ kcal/mol, while $\Delta T(H) = 0.2$ kcal/mol.

The geometry changes encountered in the reaction FE → E result in a decrease of only 0.1 kcal/mol in the total energy. However, the relaxation in the geometry, particularly the lengthening of the C–C internuclear separation, causes sizable changes in the potential energy contributions, primarily those of the carbon atoms. The contribution from the nuclear virial vanishes in reaching this metastable geometry, and the attractive and repulsive potential energy contributions change in the direction dictated by case I for the partial unmaking of the C–C bond, with $\Delta V_a > 0$ and $\Delta V_r < 0$. the kinetic energy undergoes a decrease that, aside from the small ΔE value, equals the loss of the nuclear virial. The value of $\Delta T(H)$ is only 0.1 kcal/mol for this change, showing that essentially the whole of the decrease in T comes from the carbon atom contributions. Thus, the energy increase associated with the rigid rotation of one methyl with respect to another to give the frozen eclipsed geometry arises from the contribution of the virials of the repulsive forces generated on the carbon nuclei, and this change in energy overides the decrease in the potential energy V.

One can investigate further the nature of the changes in the charge density over the basins of the carbon atoms to better understand the accompanying changes in energy. The first moment of an atom is defined as

$$\mu(\Omega) = -e\int_\Omega \mathbf{r}_\Omega \rho(\mathbf{r})\, d\tau \tag{5}$$

where the position vector $\mathbf{r}_\Omega$ is defined with the nucleus of Ω as origin. The z component of the traceless quadrupole moment tensor for atom Ω is defined as

$$Q_{zz}(\Omega) = -e\int_\Omega (3z_\Omega^2 - r_\Omega^2)\rho(\mathbf{r})\, d\tau \tag{6}$$

In the S conformation of ethane, each carbon atom is polarized toward the other with $|\mu_z(C)| = 0.030$ au. This value decreases to 0.025 au in the FE conformation. Thus, electronic charge is shifted from the binding to the antibinding regions of the carbon nuclei[20] (where these regions are defined with respect to the carbon nuclei) when the molecule is rotated without the possibility of relaxing the C–C separation. These counterpolarizations contribute to the forces of repulsion acting on the carbon nuclei in the FE conformation. They are destroyed and replaced by an even larger polarization of each carbon atom into its binding region, $|\mu_z(C)| = 0.039$ au, when the FE conformation is allowed to relax to the force-free E conformation. The value of $Q_{zz}(\Omega)$ for a carbon atom in the S conformation is +0.031 au, a polarization that corresponds to the transfer of charge from along the C–C axis to a toruslike distribution about this axis. (For comparison, the same moment for a carbon atom in acetylene has the value of 4 au.) This moment is increased to 0.074 au in the FE conformation and undergoes a further increase to 0.092 au in the E conformation. The effect is a progressive transfer of charge density from along the C–C internuclear axis to a torus of density about this axis, a polarization that contributes to the lengthening of the C–C bond and to the shortening of the C–H bonds as occur in the E conformation.

The explanations of the barriers for S → FE and for S → E, stated in terms of the associated changes in the atomic potential and kinetic energies and in terms of the forces exerted on the nuclei, are at variance with those based on the consequences of an assumed nonorthogonality of localized C–H bond orbitals.[11,12] First, the principal physical change accompanying the internal rotation, the lengthening of the C–C internuclear separation, appears not to have been included in the model calculations. Second, as a result of the dominance of this geometry change, the principal changes in the charge distribution occur along the C–C bond path and within the basins of the carbon atoms, with

(19) Slater, J. C. *J. Chem. Phys.* **1933**, *1*, 687.

(20) Berlin, T. *J. Chem. Phys.* **1951**, *19*, 208.

only relatively small changes occurring along the C–H bond paths and within the basins of the hydrogen atoms. It is difficult to rationalize the changes in density anticipated to result from the requirements of orthogonality, in this case on the localized C–H bond orbitals, with the changes in the charge density that are found to occur. One might argue that the greater C–C separation found in the E conformation is a consequence of the exchange repulsions between the C–H bond orbitals. However, the changes in density and energy for the reaction S → FE do not correspond to those anticipated on the basis of the overlap of occupied bond orbitals, as even here the primary changes in density are along the C–C axis and within the basins of the carbon atoms, and the change in potential energy is attractive rather than repulsive. The barrier in this case, which is of almost the same size as the equilibrium barrier, results from the creation of repulsive forces on the carbon nuclei whose presence increases the total energy of the system by increasing the electronic kinetic energy of the carbon atoms. Relaxing the geometry by lengthening the C–C separation to its value in th E geometry replaces these forces of nuclear repulsion with a barrier arising from an increase in the attractive potential energy of the carbon atoms.

To understand the origin of the barrier in ethane, one must understand why the C–C bond is lengthened in the eclipsed geometry. The change S → E transforms an alternating axis of symmetry into a threefold axis. The alternating field of the protons exerted the length of the C–C axis in the Hamiltonian of the S conformation is replaced by a more pronounced field with a threefold symmetry in the Hamiltonian for the E conformation. This change in the Hamiltonian has the effect of increasing the quadrupolar polarization of the electronic charge density along the C–C axis, removing charge from this axis and concentrating it in a toruslike distribution about the axis. As a consequence, the electronic charge in the C–C binding region is less effective in binding these nuclei and the C–C separation increases. This same quadrupolar polarization slightly increases the binding of the protons.

Inversion Barriers. The A–H internuclear separations in NH_3, PH_3, H_3O^+, and H_2O decrease when the pyramidal or bent geometry is transformed into the planar or linear form, respectively, with an accompanying increase in the HAH bond angles to 120° or 180° (Table II). The approach of the protons toward the A nucleus, while resulting in a lowering of the electron–nuclear attractive potential energy (Table I) in the planar or linear geometry, leads to an even greater increase in the repulsive interactions. The inversion barrier in these molecules is thus a consequence of an increase in the repulsive interactions that outweighs an accompanying decrease in the attractive potential energy, an example of a case II energy change. Rauk et al.,[9] in the first successful calculation of the barrier in ammonia, give the same explanation for its origin. The decreases in internuclear separations in these molecules result in an increase rather than a decrease in the total energy of the system, a behavior opposite to that found for case I.

The hybridization model predicts an increase in the electronegativity of the A atom relative to hydrogen in the attainment of the planar or linear geometries. This is a consequence of the increase in the s character of its bonds to hydrogen, from sp^3 to sp^2 or from p to sp, coupled with the fact that s electrons are more tightly bound than are p electrons. On this basis, one predicts a transfer of charge from H to A to accompany the shortening of the A–H bonds in the formation of the planar or linear geometries. This prediction and the associated energetic consequences are found to be correct, as indicated by the data in Table III.

The molecular charge distributions of the pyramidal and bent molecules undergo larger perturbations during inversion or linearization as a consequence of the accompanying change in hybridization than does a charge distribution for a molecule undergoing internal rotation. This greater reorganization of the charge is reflected in the larger changes in the atomic energies, changes that are a direct measure of the extent of change in the distribution of charge over the basin of each atom. The sizable redistribution of charge caused by the change in hybridization of the N atom in attaining the planar form of ammonia is reflected in the value of $Q_{zz}(N)$ changing from −2.92 au in the pyramidal molecule to −4.15 au in the planar geometry. Table III also lists the bonded radius of hydrogen in the equilibrium geometry and the change in this radius when the barrier is attained. The shifts in the A–H interatomic surface toward the proton associated with these changes are much larger for the inversion barriers than for the rotation barrier in ethane (Figure 3). Note that the decrease in the radius of the hydrogen atom parallels the increase in the electronegativity of the A atom to which it is bonded, r_H decreasing in the order A = P, C, N, O, and O^+.

The change in the relative electronegativities of N and H and the associated changes in their stabilities resulting from the change in hybridization upon inversion have a direct parallel with the changes in the properties of the carbon and hydrogen atoms of the methylene group of a normal hydrocarbon when it is transferred to a cyclic system with geometric strain. As pointed out by Walsh[21] and by Coulson and Moffit,[22] the orbital model predicts an increase in the carbon s character of the C–H bonds of a methylene group in cyclopropane compared to the unstrained group, as a result of the decrease in the C–C–C bond angle and the associated increase in p character of the C–C bonds. The transfer of the standard transferable methylene group of the normal hydrocarbon series into the cyclopropane ring structure leads to a transfer of 0.05e from each of its hydrogens to carbon, to an opening of the HCH angle and to a shortening of the C–H bonds.[23] The increased s character and the resulting increase in population of the carbon atom lead to an increase of 15.6 kcal/mol in its stability and to a corresponding decrease of 12.6 kcal/mol in the stability of each of the hydrogen atoms. Overall, the transfer of charge within the CH_2 group leads to a 9.6 kcal/mol increase in its energy relative to the standard methylene group and to a total strain energy three times this, or 28.8 kcal/mol, a value in agreement with experiment. In the same manner, the theory successfully accounts for the strain energies in cyclobutane and cyclopentane and correctly predicts cyclohexane to be strain-free. The destabilization of the hydrogens also exceeds the stabilization of the nitrogen atom in the formation of planar ammonia. In terms of the mechanical properties of atoms, the strain energy of a methylene group in a cyclic hydrocarbon and the inversion barrier in ammonia have a common origin.

The transfer of charge from H to A is larger in the linearization of water than in the pyramidalization of ammonia, and the energy barrier and changes in atomic energies are correspondingly greater for H_2O than for NH_3. The pattern of energy changes and their contributions, however, is the same for the barrier in water as it is for the barrier in ammonia, with the hydrogens being destabilized to a greater extent than the oxygen atom is stabilized. The pattern of atomic contributions is also the same for the barrier in the hydronium ion, but the charge transfer from the hydrogens to the oxygen is considerably less than in water or ammonia. The energy changes are correspondingly smaller and more evenly matched; the destabilization of the hydrogens is predicted to exceed the stabilization of the oxygen by less than 2 kcal/mol. The small transfer of charge in this case is understandable, as the hydrogens already bear a net charge of +0.74e in the pyramidal geometry of H_3O^+ and the remaining charge density on the protons is relatively tightly bound. The repulsive contributions to the energy changes of the hydrogen atoms decrease in all these molecules, and the increase in the repulsive interactions that dominates the barriers is localized within the A atoms.

The change in $V_a°(\Omega)$—the change in the attractive interaction of the nucleus of atom Ω with its own charge density—is stabilizing for the A atom and destabilizing for the hydrogens in each of the molecules. The observation that the magnitude of the decrease in $V_a°(A)$ is considerably greater than is its increase for all the

(21) Walsh, A. D. *Nature (London)* **1947**, *159*, 167, 712.
(22) Coulson, C. A.: Moffitt, W. E. *Philos. Mag.* **1949**, *40*, 1.
(23) Wiberg, K. B.; Bader, R. F. W.; Lau, C. D. H. *J. Am. Chem. Soc.* **1987**, *109*, 1001.

hydrogens in a given molecule shows that the binding of the charge transferred to the A atom is significantly increased and is one of the principal contributors to the attractive energy contributions to the barriers in these molecules.

The phosphorus atom is slightly destabilized in the planar geometry in spite of being the recipient of a transfer of charge from the hydrogen atoms. While small changes in the charge distribution of an atom lead to small changes in its energy, it is possible that a change in the distribution can be such as to result in a near-cancellation of the changes in the attractive and repulsive contributions, as occurs for the phosphorus atom in the inversion of PH_3. This differing behavior of a second- and third-row atom can be accounted for in terms of the larger size of the latter atom. The magnitude of the decrease in the value of $V_a°$ for the second-row atoms is greater than half the total decrease in $V_a(\Omega)$ (Table III). The charge transferred to the P atom, however, is relatively less effective at stabilizing the atom, since the added density is further from the attractive force of the nucleus. There is a smaller increase in stability per added electron for P than for N or O. The diffuse nature of the phosphorus charge distribution is reflected in the very large increase in its quadrupole polarization that accompanies the transfer of charge to this atom in the attainment of the planar structure, Q_{zz}(P) changing from −4.2 to −13.1 au. The decrease in the A–H bond length in attaining the planar geometry is largest in PH_3, and this atom has the largest relative increase in its repulsive energy contributions. Both the A and H atoms are destabilized in PH_3, and the inversion barrier in this molecule is six times larger than the barrier in NH_3.

Conclusions

The observations made here regarding the changes in energy and geometry associated with internal rotations and inversions should be of general applicability. For example, the same observations apply to the origin of the barrier to internal rotation about the C–O bond in carboxylic acids and esters, as studied by Wiberg and Laidig.[24] Their calculations predict formic acid, methyl formate, acetic acid, and methyl acetate to possess a minimum energy planar Z conformation. Like the rotational barriers studied here, they find the principal geometry change associated with the attainment of the nonplanar conformation to be a lengthening of the bond about which the rotation occurs, and the barriers to arise from an increase in the attractive potential energy and in spite of a decrease in the repulsive interactions. The largest energy changes occur for the C and O atoms of the rotated bond, the carbon being stabilized and the oxygen being destabilized in the nonplanar rotamer.

The origin of the barrier for the rotation of planar formamide by 90° or 270° was also investigated.[24] This is an interesting case, as here the rotation about the C–N bond results in the pyramidalization of the N atom and its formal hybridization changes from sp^2 to sp^3. Thus, as for the inversion barriers discussed above, the N atom is found to gain electronic charge from its bonded neighbors and to increase in stability when the amide group is rotated from a nonplanar into its planar form. In this molecule, however, the destabilization of the atoms that donate charge to the N atom in the planar geometry is less than the stabilization achieved by the N atom, and the equilibrium geometry of this molecule is planar. Here again, the principal geometrical change is a lengthening of the bond about which rotation occurs (as in the inversion of ammonia, the bonds to N are shortest when its s character is greatest), and the predicted barrier of 16.0 kcal/mol is a result of an increase in the attractive potential energy and a decrease in the repulsive energies. Because of the transfer of charge from N to C that accompanies the loss of planarity, most of the lengthening of the C–N bond, which equals 0.15 au, is taken up by an increase in the bonded radius of the carbon atom, from 0.83 to 1.04 au. The resonance model accounts for the relative stability of the planar geometry by invoking a resonance structure wherein the N atom donates charge to the carbonyl oxygen atom, a resonance interaction that is lost upon rotation. The resonance model is, therefore, in direct contradiction with the hybridization model for these systems, which predicts the N to be most electronegative in the planar structure. The theory of atoms in molecules shows the resonance model to be wrong in this instance.[24] Not only is the direction of the charge transfer for N incorrect, the properties of the oxygen atom, including its geometrical parameters, are found to change by only small amounts compared to the changes undergone by the C and N atoms, the magnitude of its energy change being 20–30 times smaller. This conclusion is not some artifact of the theory of atoms in molecules. It is a result of the observation that the distribution of charge over the basin of the oxygen atom—a well-defined region of real space extending to within 0.74 au of the carbon nucleus—is only slightly perturbed by a rotation about the C–N axis. Siggel et al.[25] make the same criticism of the resonance model with regard to its explanation of the relative acidities of carboxylic acids and alcohols. The enhanced acidity of the former over the latter is accounted for by the inductive effect, as measured by spatially determined atomic populations, rather than increased resonance stabilization of the carboxylate anion.

An atomic property and its change are determined by the distribution of electronic charge and its change over the basin of the atom and are model-independent. Because of this, the theory may be used to test existing models and aid in the construction of new ones.

(24) Wiberg, K. B.; Laidig, K. E. *J. Am. Chem. Soc.* **1987**, *109*, 5935.

(25) Siggel, M. R. F.; Streitwieser, A.; Thomas, T. D. *J. Am. Chem. Soc.* **1988**, *110*, 8022.

Two Isomers of the $Li_2C_2O_2$ Molecule: An ab Initio Study

J. Cioslowski

Contribution from the Department of Chemistry and Supercomputer Computations Research Institute, Florida State University, Tallahassee, Florida 32306-3006. *Received December 4, 1989*

Abstract: Ab initio calculations at the HF/6-311G* and MP2/6-311G* levels reveal the existence of two isomers of the $Li_2C_2O_2$ molecule. The linear structure corresponds to the dilithium salt of dihydroxyacetylene. The second stable structure possesses two four-membered rings, each consisting of one lithium, one oxygen, and two carbon atoms. At both the HF and MP2 levels, the two isomers are predicted to have very close energies. The GAPT atomic charges and vibrational frequencies are calculated for both structures, and the bonding is analyzed with the aid of Bader's topological theory of atoms in molecules. The results of the theoretical calculations rationalize the recent experimental observations.

Introduction

Contrary to popular belief, urea was not the first organic compound ever synthesized from inorganic substrates and benzene was not the first aromatic compound ever isolated. In 1825, Gmelin isolated yellow dipotassium salt of crocoic acid from the material obtained by heating potassium hydroxide and carbon.[1]

0002-7863/90/1512-6536$02.50/0